79-4053

Temperature Distribution in Louvered Panels

Robert D. Karam*
Fairchild Space and Electronics Company, Germantown, Md.

The temperature distribution along a radiating panel as affected by the presence of thermal louvers is investigated. A linear relation between the effective emittance and temperature is introduced in the energy equation and the mathematical solution is found to agree numerically with the more conventional techniques employing incremental and iterational methods. Experimental results indicate the validity of the model. The analysis provides a description of the thermal features of nonisothermal louvered panels and yields convenient procedures for evaluating thermal gradients and heat-transfer rates. A numerical example is given to illustrate application of the theory.

Nomenclature

A = dimensionless parameter

$$= \left[\frac{4(\epsilon_o - \epsilon_c) L^2 \sigma T_i^3 \tau_m^3}{(\tau_o - \tau_c)\kappa t}\right]^{1/2}$$

a = slope $= (\epsilon_o - \epsilon_c)/(T_o - T_c)$
b = intercept $= (\epsilon_o T_c - \epsilon_c T_o)/(T_o - T_c)$
$E(\theta,k), F(\theta,k)$ = Jacobian elliptic function of the second and first kind, respectively
k = modulus of elliptic function
L = length
Q = heat rejected by unit width
T = absolute temperature
t = thickness
x = distance
α = dimensionless slope $= b/aT_i$
β = dimensionless parameter

$$= \left[\frac{(\epsilon_o - \epsilon_c) L^2 \sigma T_i^4}{(T_o - T_c)\kappa t}\right]^{1/2}$$

γ = $\alpha - 0.75\,\tau_m$
ϵ = emittance
η = $\tau - \alpha$
θ = argument of elliptic function
κ = conductivity
λ = scaling factor of elliptic function
ξ = dimensionless distance
σ = Stefan-Boltzmann constant
τ = dimensionless temperature

Subscripts

l = end of panel
i = initial position
m = mean value
o,c = values for open and closed louvers

Introduction

THERMAL louvers are utilized on spacecraft as a device for active temperature control when heat dissipation from electronic equipment varies widely. A louver set of the type used on ATS-6 is shown in Fig. 1. Similar louvers have flown on numerous other satellites including the Nimbus and Mariner series. They are presently being used in the Multimission Modular Spacecraft (MMS) design as the primary system for thermal control.

Louvers consist of a framed array of highly polished blades which are individually pivoted to temperature-sensitive actuators. The actuators may be bimetallic coil springs enclosed within a housing which is well isolated from the external environment but which maintains good thermal contact with the mounting panel requiring thermal control. The actuators are "calibrated" to cause the associated blades to be fully open and fully closed at prescribed temperatures. As the temperature of the panel begins to increase, the related rise in the actuators' temperature creates a thermal moment which forces the louver blades to open and hence lead to an increase in the radiative power to space. Similarly, as the panel temperature decreases, the actuators tend to close the blades which now offer a high resistance to radiation losses. The range of radiative capability between the open and closed blade positions in currently available louvers can accommodate a one to seven thermal power variation within a temperature span of about 15 K.

The radiative capability as a function of temperature (or blade opening angle) is related to an "effective emittance" which may be defined as the ratio of the net heat transfer from a louvered surface to the energy that would be radiated from an equivalent black area at the same temperature but in the absence of louvers. In one of the earlier works on the

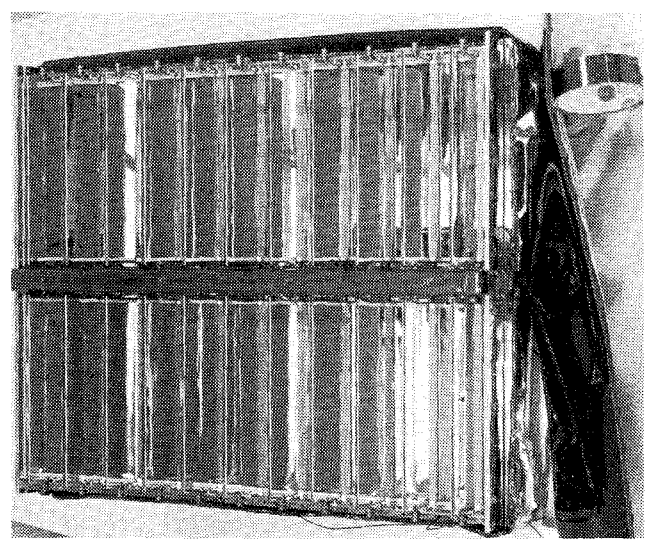

Fig. 1 ATS-6 development louvers (test configuration – optical solar reflector panel).

Received June 26, 1978; revision received Sept. 19, 1978.

Index categories: Spacecraft Temperature Control; Radiation and Radiative Heat Transfer.

*Principal Engineer, Thermal Control.

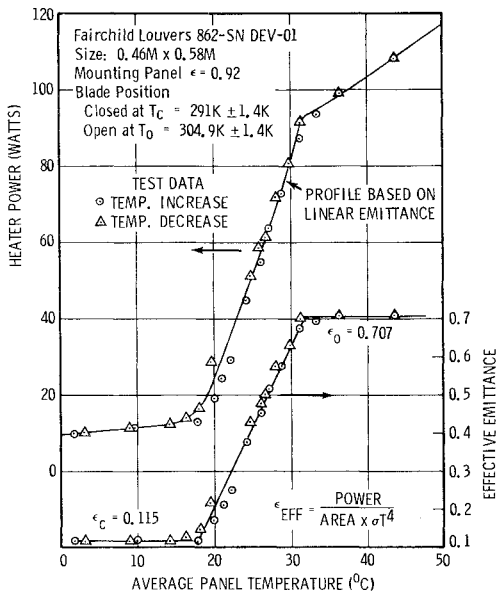

Fig. 2 Louvers' performance data.

thermal characteristics of louvers, Plamondon[1] considered an isothermal panel and established the equations which connect the effective emittance to the thermal properties and blade geometry. Parmer and Buskirk[2,3] and Parmer and Stipandic[4] extended the analysis to include specular blades and external heat inputs due to direct solar impingement or blockage by a sun-protective shield. The mathematical models have compared favorably with results of tests directed to finding effective emittance and absorptance as functions of blade angle and solar incidence angle.[5-7] The numerical data obtained from these tests form the basic input to the problem of finding the temperature of a louvered panel corresponding to a particular dissipation and solar environment. A typical variation of emittance with temperature and the corresponding power profile are shown in Fig. 2.

The emphasis has generally been placed on isothermal louvered panels. Usually, however, spacecraft panels are not isothermal, although louvers can serve to reduce thermal gradients without sacrificing the required levels of operating temperatures. This paper presents a study of the temperature distribution as affected by boundary conditions and the thermal characteristics of the louvers and associated panel. The validity of the analysis is confimed by comparison with conventional numerical methods and test data. An example is given to demonstrate application to preliminary design studies.

Analysis

A schematic of the physical situation is shown in Fig. 3. One-dimensional steady-state conduction in the direction of the axis of the actuator housing is considered with the indicated boundary conditions which are suggested by typical spacecraft panels employing louvers.[8] No external heat sources are present, and all extraneous heat losses by conduction and radiation are considered minor and inherent in the value of effective emittance $\epsilon(T)$, which is a predetermined function of temperature. The system is assumed to be operating within the temperature range at which the louvers are calibrated, and the energy equation is given by

$$\frac{d^2T}{dx^2} = \frac{\epsilon(T)}{\kappa l}\sigma T^4 \tag{1}$$

with

$$T(0) = T_i \qquad (dT/dx)_{x=L} = 0 \tag{2}$$

The dependence of ϵ on temperature is assumed as follows:

$$\epsilon(T) = \epsilon_c \text{ (constant)} \qquad (T \le T_c) \tag{3}$$

$$\epsilon(T) = aT - b \qquad (T_c \le T \le T_o) \tag{4}$$

$$\epsilon(T) = \epsilon_o \text{ (constant)} \qquad (T \ge T_o) \tag{5}$$

a and b are determined from the properties of the louvers and calibration limits T_c and T_o,

$$a = (\epsilon_o - \epsilon_c)/(T_o - T_c) \tag{6}$$

$$b = (\epsilon_o T_c - \epsilon_c T_o)/(T_o - T_c) \tag{7}$$

The form of emittance as defined in Eqs. (3) and (5) is consistent with known test data (see, for example, Refs. 1, 5, 6 and 7). The spread of test data points for isothermal panels in the region $T_c \le T \le T_o$ can be generally contained within two nearly parallel lines which bound the louvers performance and account for unpredictable frictional effects. Hence, a linear profile as given by Eq. (4) may be justified if the panel carries a sufficient number of blades or if the temperature variation is not so large as to make the angular position of a blade much different from that of an adjacent one. In actual practice, strength and weight considerations in louvers design lead to minimizing the height of the relatively heavy frames and actuator housing, which in turn limit the width of blades in order to avoid interference with the mounting panel. Usually, therefore, a large louver set contains many blades spaced within short distances. On the other hand, short panels controlled by small sized louvers having few blades inherently exhibit small temperature gradients.

T^4 in Eq. (1) is approximated by the first two terms of a Taylor expansion about a mean temperature T_m; that is,

$$T^4 \approx T_m^4 + 4T_m^3(T - T_m) \tag{8}$$

where T_m is determined in view of minimizing the error in the approximate solution.[9] Equation (1) in dimensionless form becomes

$$\frac{d^2\tau}{d\xi^2} = A^2(\tau - \alpha)(\tau - 0.75\,\tau_m) \tag{9}$$

with

$$\tau(0) = 1 \quad \text{and} \quad (d\tau/d\xi)_{\xi=1} = 0 \tag{10}$$

where

$$\tau = T/T_i \qquad \xi = x/L$$

$$A^2 = 4(\epsilon_o - \epsilon_c)L^2\sigma T_i^3\tau_m^3/(\tau_o - \tau_c)\kappa l$$

$$\alpha = (\epsilon_o\tau_c - \epsilon_c\tau_o)/(\epsilon_o - \epsilon_c)$$

The integral of Eq. (9) is represented by

$$\sqrt{2/3}A(1-\xi) = \int_{\eta_1}^{\eta} \frac{d\eta}{[(\eta-\eta_1)(\eta-\eta_2)(\eta-\eta_3)]^{1/3}} \tag{11}$$

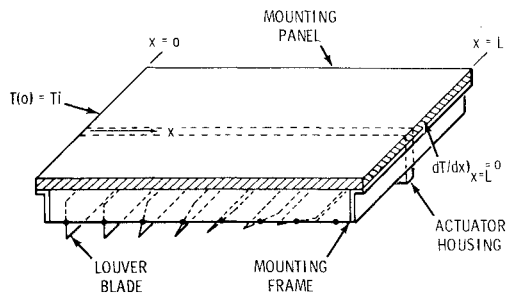

Fig. 3 Louvered panel math model.

where $\eta = \tau - \alpha$ and η_1, η_2, and η_3 are the roots of

$$\eta^3 + \frac{3}{2}\gamma\eta^2 - \left(\eta_1^3 + \frac{3}{2}\gamma\eta_1^2\right) = 0 \tag{12}$$

$\eta_1 = \tau_1 - \alpha$, where τ_1 is the dimensionless temperature at the adiabatic end of the panel ($\xi = 1$), and $\gamma = \alpha - 0.75\ \tau_m$. The two remaining roots, η_2 and η_3 are given by

$$\eta_{2,3} = \frac{1}{2}\left\{-\left(\eta_1 + \frac{3}{2}\gamma\right) \pm \left[\left(\eta_1 + \frac{3}{2}\gamma\right)^2 - 4\eta_1\left(\eta_1 + \frac{3}{2}\gamma\right)\right]^{1/2}\right\} \tag{13}$$

Equation (11) is an elliptic integral of the first kind whose numerical value depends on the nature of the roots in Eq. (12). For a reasonably designed louvers set, T_o/T_c is about unity, while ϵ_o/ϵ_c is 6 or greater. From this follows that both η and γ are positive and therefore when $0 < \eta_1 \leq \gamma/2$ the roots in Eq. (12) are all real and lie in the order $\eta_1 > \eta_2 > \eta_3$. The radical in Eq. (13) is complex when $\eta_1 > \gamma/2$ and the only real root is η_1. Equation (11) in standard form is written[10]

$$\sqrt{2/3}A(1-\xi) = (1/\lambda)F[\theta(\eta),k] \tag{14}$$

F being the elliptic function of the first kind and λ, θ, and k are defined as follows:

$$\lambda = \tfrac{1}{2}(\eta_1 - \eta_3)^{1/2}$$

$$\theta(\eta) = \sin^{-1}\left(\frac{\eta - \eta_1}{\eta - \eta_2}\right)^{1/2}$$

$$k = \left(\frac{\eta_2 - \eta_3}{\eta_1 - \eta_3}\right)^{1/2}$$

for $0 < \eta_1 \leq \gamma/2$; and

$$\lambda = (3\eta_1^2 + 3\gamma\eta_1)^{1/4}$$

$$\theta(\eta) = \cos^{-1}\left(\frac{\lambda^2 + \eta_1 - \eta}{\lambda^2 - \eta_1 + \eta}\right)$$

$$k = \left(0.5 - \frac{1}{8}\frac{6\eta_1 + 3\gamma}{\lambda^2}\right)^{1/2}$$

for $\eta_1 > \gamma/2$. Using the condition $\eta(0) = 1 - \alpha$, the temperature distribution along the panel, Eq. (14), can be written as

$$\xi = 1 - F[\theta(\eta),k]/F[\theta(1-\alpha),k] \tag{15}$$

Also

$$\sqrt{8/3}\beta\tau_m^{3/2} = (1/\lambda)F[\theta(1-\alpha),k] \tag{16}$$

where

$$\beta^2 = (\epsilon_o - \epsilon_c)L^2\sigma T_i^4/(T_o - T_c)\kappa t$$

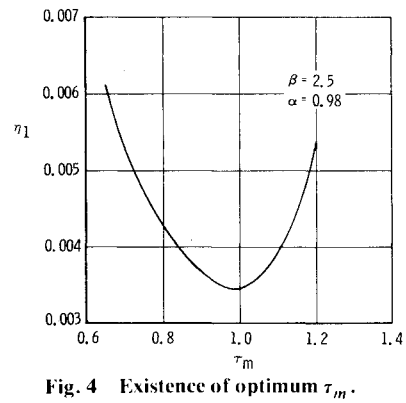

Fig. 4 Existence of optimum τ_m.

Equation (16) relates the end temperature τ_1 to known parameters and mean temperature.

The dimensionless mean temperature τ_m can be selected in accordance with the requirement that the error introduced in using Eq. (15) be minimized. Since

$$\tau^4 > \tau_m^4 + 4\tau_m^3(\tau - \tau_m)$$

the values of temperature obtained from the solution of Eq. (9) can be made only to approach the exact values by the appropriate selection of τ_m. Figure 4 illustrates the variation of η_1 with τ_m as given by Eq. (16). The optimum value of τ_1 is an excellent estimate of the actual temperature and is found from the constraint

$$\frac{\partial\tau_1}{\partial\tau_m} = \frac{\partial\eta_1}{\partial\tau_m} = 0 \tag{17}$$

Noting that[11]

$$\left(\frac{\partial F}{\partial\theta}\right)_k = (1 - k^2\sin^2\theta)^{-1/2}$$

and

$$\left(\frac{\partial F}{\partial k}\right)_\theta = \frac{E(\theta,k) - (1-k^2)F(\theta,k)}{k(1-k^2)} - \frac{k\sin\theta\cos\theta}{(1-k^2)(1-k^2\sin^2\theta)^{1/2}}$$

where $E(\theta,k)$ is the elliptic function of the second kind, differentiation of both sides of Eq. (16) with respect to τ_m and subject to Eq. (17) yields

$$\sqrt{8/3}\,\beta\left[\frac{3}{4}(\eta_1 - \eta_3)^{1/2}\tau_m^{1/2} - \frac{1}{4}(\eta_1 - \eta_3)^{-1/2}\tau_m^{3/2}\eta_3'\right]$$

$$= \frac{\tan\theta}{(1-k^2\sin^2\theta)^{1/2}(1-\alpha-\eta_2)}\left[\frac{9}{32} + \frac{1}{4}(\eta_2' - \eta_3')\right]$$

$$+ \left[\frac{E(\theta,k) - (1-k^2)F(\theta,k)}{k(1-k^2)} - \frac{k\sin\theta\cos\theta}{(1-k^2)(1-k^2\sin^2\theta)^{1/2}}\right]$$

$$\times\left[\frac{\eta_2' - (1-k^2)\eta_3'}{2k(\eta_1 - \eta_3)}\right] \tag{18}$$

for $\eta_1 \leq \gamma/2$. The values of η_2' and η_3' are given by

$$\eta_{2,3}' = \frac{9}{16}\left[1 \pm \frac{\eta_1 - (3/2)\gamma}{\{[\eta_1 + (3/2)\gamma]^2 - 4\eta_1[\eta_1 + (3/2)\gamma]\}^{1/2}}\right] \tag{19}$$

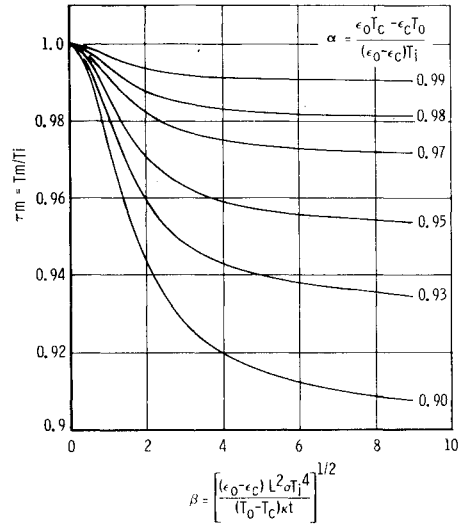

Fig. 5 Optimum mean temperature.

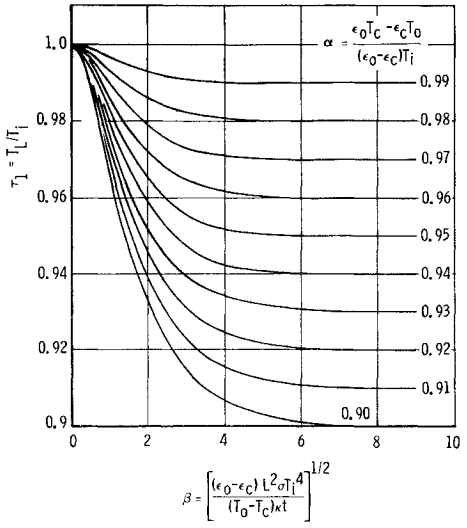

Fig. 6 End temperature vs louvers/panel parameters.

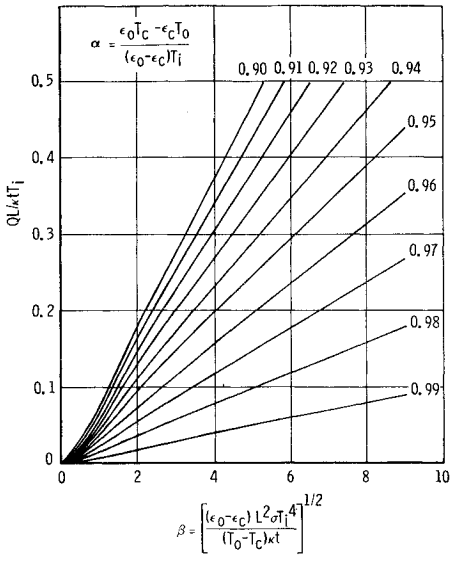

Fig. 7 Heat rejected vs louvers/panel parameters.

Similarly, for $\eta_1 > \gamma/2$

$$\sqrt{8/3}\,\beta\left(\frac{3}{2}\lambda\tau_m^{1/2} - \frac{9}{16}\eta_1\frac{\tau_m^{3/2}}{\lambda^3}\right)$$

$$= \frac{9}{8}\frac{\eta_1(1-\cos\theta)}{\lambda^2(\lambda^2+1-\alpha-\eta_1)(1-k^2\sin^2\theta)^{1/2}\sin\theta}$$

$$+ \frac{9}{64}\left[\frac{E(\theta,k)-(1-k^2)F(\theta,k)}{k(1-k^2)} - \frac{k\sin\theta\cos\theta}{(1-k^2)(1-k^2\sin^2\theta)^{1/2}}\right]$$

$$\times\left[\frac{1-0.5\eta_1(6\eta_1+3\gamma)/\lambda^6}{k\lambda^2}\right] \qquad (20)$$

Equation (18) or (20) and Eq. (16) form two simultaneous equations in optimum τ_m and the corresponding $\tau_1 = \eta_1 + \alpha$. A numerical solution can be obtained by iterating on the value of τ_1 which, for a fixed τ_m, gives the same β in both equations. The results are shown in Figs. 5 and 6. The value of α generally encountered in practice ranges from about 0.90 to slightly less than 1.0.

The heat rate rejected by the panel is equivalent to the amount conducted at $x = 0$; that is

$$Q = -\kappa t\left(\frac{dT}{dx}\right)_{x=0} \qquad (21)$$

where Q is heat rejected per unit panel width. Equation (1) can be written as

$$d\left(\frac{d\tau}{d\xi}\right)^2 = \frac{2aL^2\sigma T_i^4}{\kappa t}(\tau-\alpha)\tau^4 d\tau \qquad (22)$$

Hence, by integrating Eq. (22) and substituting Eq. (21),

$$\frac{QL}{\kappa t T_i} = \beta[(1/3)(1-\tau_1^6) - (2\alpha/5)(1-\tau_1^5)]^{1/2} \qquad (23)$$

Equation (23) is represented by the curves of Fig. 7 which incorporate the best estimate for τ_1.

The results obtained from Eqs. (16) and (23) are predicated on the assumption that the temperature along the panel is confined between the louvers calibration limits T_c and T_o so that Eq. (4) remains valid. This places a constraint on the amount and range of heat rejected by a louvered panel if the system is to be maintained between T_c and T_o. Figures 6 and 7 can be used together to determine the temperature at the end of the panel and the heat output as they vary with the temperature at $x = 0$. The restrictions that $T_i \le T_o$ and $T(L) \ge T_c$ determine the bounds on heat rejection capability as a function of systems' parameters.

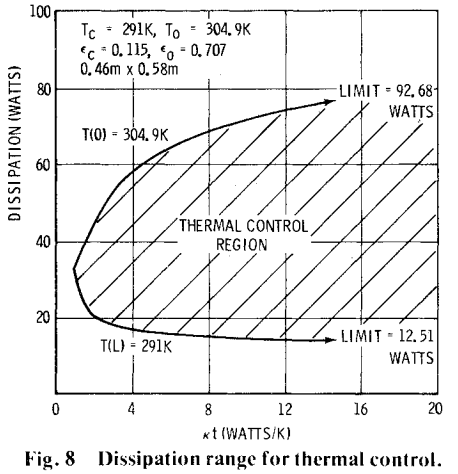

Fig. 8 Dissipation range for thermal control.

Numerical Example

As an example, consider the thermal control of a dissipating component located on one end of a louvered panel whose characteristics are as indicated in Fig. 2:

$T_c = 291.0$ K $\quad \epsilon_c = 0.115$

$T_o = 304.9$ K $\quad \epsilon_o = 0.707$

L $= 0.58$ m $\quad$ width $= 0.46$ m

Here $\alpha = 288.3/T_i$ and $\beta = 2.872 \times 10^{-5} T_i^2/\sqrt{\kappa t}$ where T_i is temperature in degrees Kelvin at $x = 0$ and κt is conductivity-thickness product in W/K. Parameters α and β are calculated for various T_i and known κt, and Fig. 6 is used to obtain the corresponding temperature at the end of the panel. Sample calculations are given in Table 1. The result is meaningful only if $T(L) \ge 291.0$ K, in which case heat rejection rate is found from Fig. 7 or, more conveniently, from Eq. (22). The final results are represented in Fig. 8. It is seen that temperature control within the calibration limits is not possible for κt less than 0.989 W/K. At this value and a dissipation of 32.9 W the temperature spans the whole control range of 304.9 K at $x = 0$ to 291.0 K at $x = 58$ cm. The range of dissipation which can be accommodated widens as κt in-

Table 1 Dissipation range for thermal control (sample calculations)[a]

κt, W/K	T_i, K	β	α	τ_l (Fig. 6)	$T(L)=\tau_l T_i$, K	$QL/\kappa t T_i$ (Eq. 23)	$Q\times$width, W
0.9889	304.9	2.6847	0.9456	0.9544	291	0.139	32.9
10.00	304.9	0.8443	0.9456	0.9870	300.6	0.029	71.2
	295	0.7904	0.9773	0.9947	293.4	0.018	43.1
	293	0.7797	0.9840	0.9961	291.9	0.008	18.9
	292	0.7744	0.9873	0.9970	291.1	0.0063	14.6
	291.88	0.7737	0.9877	0.9971	291.0	0.0061	14.1

[a] $T_c=291$ K, $T_o=304.9$ K, $\epsilon_c=0.115$, $\epsilon_o=0.707$, 0.46 m × 0.58 m.

creases. The limiting values (12.51 W min. and 92.68 W max.) are those for an isothermal panel. By contrast, a panel without louvers which has the same area, a constant emittance of 0.25 and $\kappa t=1.7$ W/K rejects about the same amount of heat when the boundary temperatures are 304.9 K and 291.0 K. However, in this case, very limited compensation for temperature sensitivity to power change can be provided by increasing κt. The maximum and minimum permissible dissipations which will maintain the system within the required temperatures are found for an isothermal panel to be 33 W and 27 W, respectively.

For $T_i=304.9$ K and $\kappa t=0.989$ W/K, $\beta=2.6847$ and $\alpha=0.9456$. Hence, from Fig. 6, $\tau_l=0.9544$ or $T(L)=291$ K. Figure 7 gives $\tau_m=0.962$. The value of $\eta_l=\tau_l-\alpha=0.0088$ and $\gamma=\alpha-0.75\tau_m=0.2241$. Since $\eta_l<\gamma/2$, the other two roots of Eq. (12) are real with $\eta_2=-0.0090$ and $\eta_3=-0.3359$. Also $\lambda=0.2935$, $k=0.9738$, and $\theta(1-\alpha)=57.97$ deg. The value of $F(57.97\text{ deg}, 0.9738)$ is computed or found from the tables[10] to be 1.2267. Hence Eq. (15) becomes

$$\xi=1-F(\theta,0.9738)/1.2267 \tag{24}$$

Equation (24) is solved by selecting θ and finding the corresponding ξ. The results in terms of T vs x are shown in Fig. 9. The sensitivity to τ_m was examined by repeating the calculations for $\tau_m=0.9$, 0.962, and 1.0. No significant differences were observed provided the optimum $\tau_l=0.9544$ was used. Comparison with the results of a 24 node thermal model for Systems Improved Numerical Differencing Analyzer (SINDA) computer program which iterates on nonlinear radiation showed almost identical values. This affirms the accuracy of the analytical method when the magnitude of gradients is of practical order. Figure 9 also shows the temperature distribution in the absence of louvers and 0.35 emittance ($\kappa t=0.989$ W/K). The equation used is obtained from the analysis in Ref. 9 and is given by

$$\tau(\xi)=0.705+0.22\cosh 0.8038(1-\xi) \tag{25}$$

Test Verification

The louvers data in the preceding example derive from tests conducted on a development unit (Fig. 1) which was manufactured for ATS-6 application. The blade shafts and the cover for the actuators housing were nonmetallic, which tended to minimize space environment effects on the actuators, and a narrow stripe of white paint on each blade prevented excessive solar heating. The set carried 11 pairs of 6-cm × 20-cm blades which, together with the actuators housing, were enclosed by a frame that covered a total area of 0.46 m × 0.58 m. Motion of blade pairs was activated by the temperature response of individual bimetallic spiral springs inside the insulated housing. A meticulous procedure was exercised in selecting the springs in order to insure uniformity of blades' angular positions. Heat exchange between the actuators and the mounting panel was enhanced by employing a blackening process on the springs and thermally conductive grease at the housing surface which mates with the panel.

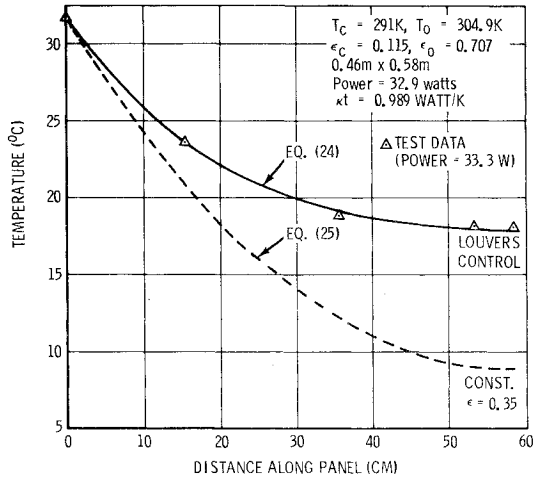

Fig. 9 Temperature distribution.

The assembly was calibrated at normal pressure in an air chamber equipped with temperature controllers. The blades had accompanying protractors which registered angular position as a function of air temperature. Ten steady-state positions, including fully closed and fully open, were established at 10-deg intervals and then secured by adjustment screws which varied the tension in the springs. The procedure was repeated until angular uniformity within 1 deg was achieved among the blades. All of the blades were closed at air temperature less or equal to 289K (±0.5 K) and fully open at greater or equal to 303 K (±0.5 K).

Effective emittance tests using various types of radiator panels were conducted in a cryogenic vacuum chamber (10^{-6} Torr) 2 m in diameter and 2.13 m long. Heaters with controlled power were bonded to the backside of the panel and covered with multilayer superinsulation. The insulation extended over the panel edges and outer surface of the louvers frame. Evenly distributed thermocouples were installed on the panel for monitoring the temperature, and all wiring was collected into a single bundle wrapped in thin aluminized mylar sheets to minimize heat losses. The assembly was suspended in the chamber by stainless steel wires, and the tests performed in accordance with standard procedures.[6] Steady-state conditions were achieved for a series of power levels, and the temperatures were monitored and recorded. The data were corrected to account for predictable losses and gains, and the effective emittance was calculated as the ratio of the net power radiated by the louvers to the ideal power which would be radiated by an equivalent black area at the same temperature.

$$\text{effective emittance}=\frac{\text{net heat radiated by louvered surface}}{\text{area enclosed by frame}\times\sigma T^4}$$

Typical results are shown in Fig. 2. It was noted by comparison with calibration data that a temperature differential of about 2 K existed between the panel and the actuators. This

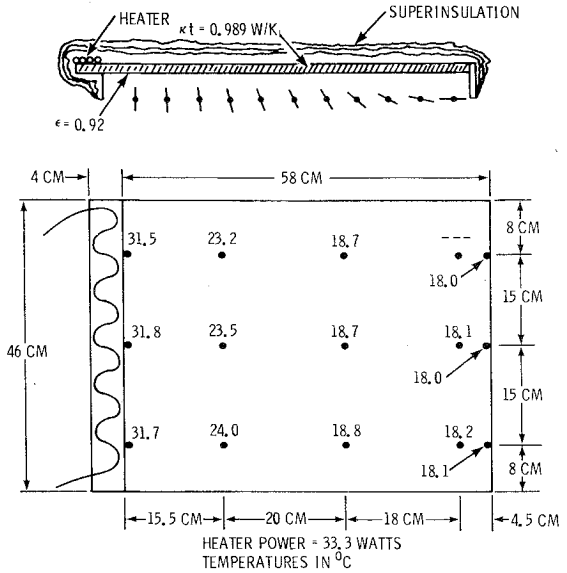

Fig. 10 Conduction test configuration and results.

was an indication that environmental effects could not be completely eliminated and spacecraft thermal design must consider this lag.

One of the panels was selected in preparation for the longitudinal conduction tests. This was a 0.635-cm thick 6061-T4 aluminum ($\kappa = 1.557$W/cm-K) coated with black ($\epsilon = 0.92$). The length extended 4 cm beyond the louvers frame to provide space for installing a side heater to simulate a dissipating component located at one end. The heater power could be manipulated to achieve the desired temperature at the initial position. The configuration is shown schematically in Fig. 10. The assembly was suspended in the vacuum chamber with its back facing the insulated surface of a second louvers assembly undergoing independent testing. This arrangement practically eliminated heat losses through the insulation.

A steady-state average temperature of 305 K (31.7°C) was produced at the initial position by dissipating 33.3 W in the side heater. Steady state was assumed to exist when variations of less than 0.1 K/h were observed. The final temperature distribution is shown in Fig. 10. The lateral arithmetic averages were found to correlate very well with the analytical results. The comparison is indicated in Fig. 9. A significant conclusion is that the assumption of a linear variation of emittance with the temperature of a conducting louvered panel is valid.

Acknowledgments

The author wishes to thank A. Boscia and C. Colaluca of Fairchild Test Group for their help in designing and executing the test.

References

[1] Plamondon, J.A., "Analysis of Moveable Louvers for Temperature Control," *Journal of Spacecraft and Rockets,* Vol. 1, Sept.-Oct. 1964, p. 92.

[2] Parmer, J.F. and Buskirk, D.L., "The Thermal Radiation Characteristics of Spacecraft Temperature Control Louvers in the Solar Space Environment," AIAA Paper 67-307, New Orleans, La., April 1967.

[3] Parmer, J.F. and Buskirk, D.L., "Thermal Control Characteristics of Interior Louver Panels," ASME Paper 67-HT-64, Seattle, Wash., Aug 1967.

[4] Parmer, J.F. and Stipandic, E.L., "Thermal Control Characteristics of a Diffuse Blade, Specular Base Louver System," AIAA Paper 68-764, 3rd Thermophysics Conference, Los Angeles, Calif., 1968.

[5] Clausen, O.W. and Kirkpatrick, J.P., "Thermal Tests of an Improved Louver System for Spacecraft Thermal Control," AIAA Paper 69-627, 4th Thermophysics Conference, San Francisco, Calif., June 1969.

[6] Boscia, A.J., "A Laboratory Method for the Determination of Effective Emittance of Spacecraft Thermal Control Louvers," Paper VIC. 3, Joint National Meeting of American Astronautical Society (15th Annual) and Operations Research Society (35th National), Denver, Colo., June 17-20, 1969.

[7] Michalek, T.J., Stipandic, E.A., and Coyle, M.J., "Analytical and Experimental Studies of an All Specular Thermal Control Louver System in a Solar Vacuum Enviroment," AIAA Paper 72-268, 7th Thermophysics Conference, San Antonio, Texas, 1972.

[8] Eby, R.J., Kelly, W.H., and Karam, R.D., "Thermal Control of ATS F&G," ASME Paper 71-Av-28, SAE/ASME/AIAA Life Support and Environmental Control Conference, San Francisco, Calif., July 12-14, 1971.

[9] Karam, R.D. and Eby, R.J., "Linearized Solution of Conducting-Radiating Fins," *AIAA Journal,* Vol. 16, May 1978, pp. 536-538.

[10] Abramowitz, M. and Stegun, I.A. (eds.), *Handbook of Mathematical Functions with Formulas, Graphs, and Mathematical Tables,* National Bureau of Standards, AMS 55, U.S. Government Printing Office, Washington, D.C., June 1964, Chap. 17, pp. 589-626.

[11] Byrd, P.F. and Friedman, M.D., *Handbook of Elliptic Integrals for Engineers and Physicists,* Springer-Verlag, Berlin, 1954, formulas 710.07 and 730.00.